

# Modeling, Fabrication and Experiment of a Novel Lateral MEMS IF/RF Filter

Mehrnaz Motiee\*, Amir Khajepour\* and Raafat R. Mansour\*\*

University of Waterloo, Waterloo, Ontario, Canada

\*Mechanical Eng. Dept., mehrnaz@mems.uwaterloo.ca, akhajepour@uwaterloo.ca

\*\*Electrical and Computer Eng. Dept., rmansour@maxwell.uwaterloo.ca

## ABSTRACT

MEMS based mechanical resonators and filters have shown promising characteristics in achieving high Q values and good stability. This paper introduces a novel V-shape coupling element that is used to mechanically couple two clamped-clamped MEMS resonators laterally. The stiffness of the proposed V-shape coupling element is adjustable via changing the length of the V sidelines and/or the V conjunction angle to flatten the filter passband. In previous literature, only a single resonator in lateral vibration is considered. No suggestions were given on the coupling of such type of resonators. In this work a V-shape coupling and two beam elements are used to construct a 2-pole bandpass filter operating in the intermediate frequency (IF) range. It is fabricated using the PolyMUMPs process. A lumped modeling approach is presented, which allows a fast and accurate modeling and optimizing of the structures. With the help of finite element analysis, the validity and accuracy of the lumped modeling is investigated. Filters have been fabricated and tested. Presented filters have center frequencies varying from 700 kHz to 1.7 MHz, quality factors of 300 to 1500 when tested in a non-vacuum chamber.

**Keywords:** RF MEMS, Bandpass Filters, MUMPs, Intermediate Frequency MEMS.

## 1 INTRODUCTION

Currently, the global interest in the wireless communication field demands the integration of RF transceivers on a single silicon chip [1,2]. Filters have a major role in the construction of high performance transceivers. Bandpass filters are one of the most important elements in frequency selective circuits. This paper introduces a novel V-shape coupling element that is used to mechanically couple two clamped-clamped MEMS resonators in lateral vibration, as shown in Figure 1. The V-shaped coupling element imparts the vibrational energy from the input resonator to the output resonator by compression and expansion. In [2], only a single resonator in lateral vibration is considered. No suggestions were given on the lateral vibrating coupling elements.

The stiffness of the proposed V-shape coupling element is adjustable via changing the length of the V sidelines and/or the V conjunction angle to flatten the filter passband.

Figure 2 shows a picture of the fabricated chip. It is fabricated using the PolyMUMPs process [3].

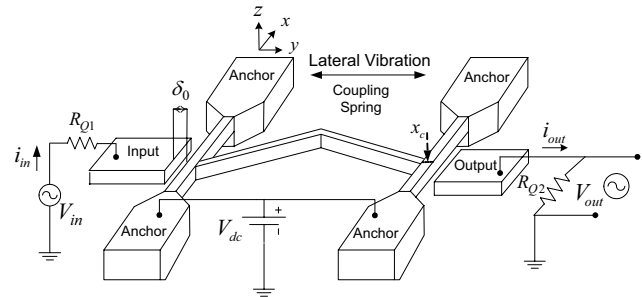


Figure 1: Schematic of a two-resonator filter with a typical measurement circuit.

Due to the multi-domain operation of these structures, a fast and accurate design tool, using general lumped modeling approach is needed. This model should include the effects of distributed and multi-domain nature of MEMS filters. In this paper, we present a lumped-element model for the modeling and design of such type of MEMS filters. The model is developed using direct electromechanical analogy [4]. It has been used for primary simulation and parametric optimization of the design. The accuracy of this model has been verified by comparing its result with finite element results. An excellence agreement between the lumped and the finite element analysis show the applicability of the lumped model to MEMS filter analysis and design. The comparison between simulation and test results under air damping is presented.

## 2 DESIGN CONCEPT AND OPERATION

Figure 1 presents a two-resonator filter, along with appropriate bias, excitation and input-output circuitries.

The conductive electrodes serve as capacitive transducer electrodes to induce resonator vibration in lateral, parallel with substrate, direction. A  $2 \mu\text{m}$  resonator to electrode gap,  $\delta_0$ , is used. To operate this filter, a *dc* voltage is applied to the suspended filter structure, which is called *dc*-bias voltage,  $V_{dc}$ , while an *ac* input voltage,  $V_{in}$ , is applied through resistor  $R_{Q1}$  to the input electrode, as shown in Fig. 1. The application of this input creates an electrostatic force in *y* direction and when the frequency of the input voltage reaches the first natural frequency of the resonator, the beam shows maximum oscillation amplitude.

As the frequency of the input voltage increases, the resonator beam intends to vibrate in its second mode of vibration. However, according to selected mode excitation theory [5], the straight-line electrode shape mainly excites the first mode and the first natural frequency becomes the dominant mode of vibration. This vibration energy is imparted to the output resonator via the coupling spring. Vibration of the output resonator creates a time varying capacitor between the conductive resonator and output electrode, which sources an output current that causes a variable output voltage,  $V_{out}$ .

### 3 MATHEMATICAL MODELING

Following is a lumped modeling approach, including the effects of the distributed and multi-domain nature of the problem. At each step, the results are compared with FEM simulation from CoventorWare [6] software to verify the model.

#### 3.1 Resonator Design

Figure 3(a) shows the schematic of a single beam resonator in lateral vibration. The natural frequency of this clamped-clamped beam resonator is not dependent on its thickness,  $T$ . Assuming the first mode, frequency vs. dimensions can be plotted in a contour plot as shown in Fig. 4(a), which defines the center frequency of the resonator with respect to  $W$  and  $L$  [4].

We have selected two different beams for two different ranges of frequencies. The dimensions of the beams and their center frequencies are given in Table 1.

For the filter design, it is more convenient to define an equivalent lumped parameter mass-spring-damper mechanical circuit for this resonator. Knowing the frequency of the beam and its first mode shape, using the energy equations, its equivalent lumped mass, stiffness and damping parameters at any location  $x$  along the beam length are found [7].

#### 3.2 Electro-mechanical operation

The electrostatic force between the resonator and electrode is nonlinear. Assuming small vibration amplitude, the force equation is linearized around its operation point with respect to voltage and displacement. As a result, an extra term with negative sign in the stiffness part arises, which is called electrical spring, denoted with  $K'$ . The total stiffness of the resonator,  $K_e(x)$ , is the summation of  $K(x)$  and  $K'$ , which decreases the total stiffness [7]. The center frequency is shifted due to electrical stiffness. The shifted original and frequencies are listed in Table 2.

Also there is a transformer coefficient between force  $F$  and the voltage  $V$ , which illustrates the energy transformation between mechanical and electrical domain.

This is called electromechanical transformer ratio, denoted by  $\eta$ . The  $\eta$  strongly depends on gap spacing  $\delta_0$  [4].

With direct analogy, mechanical lumped parameters are transferred to electrical domain to form the electrical circuit shown in Fig. 5. Calculated lumped parameters for Beam1 and Beam2 are listed in Table 3.

#### 3.3 Stability and Pull-in Voltage Analysis

The operation of the filter introduced above is based on applying a  $dc$ -bias voltage to the initial gap between the resonator and electrode to pull down the beam to its stable equilibrium position. The resonator is at stable equilibrium position if

$$K > K' \quad (1)$$

Eq. (1) can be solved for the proper  $dc$ -bias voltage. The effect of distributed electrical stiffness is considered by writing the electrical stiffness on a small differential element of the beam and integrating it over the electrode width [4]. Clearly, with increasing the voltage there will be a specific point at which the stability of the equilibrium is lost and structure collapses toward substrate. This is called *pull-in* voltage, denoted by  $V_{PI}$ . At the pull-in voltage:

$$K' = K \quad (2)$$

Figure 6 shows the pictures of fabricated Beam1 in neutral and pull-in positions. When the pull-in voltage is known, the deflection of the beam for Beam1 and Beam 2 can be calculated from, [7]:

$$y_{PI}(x) = \delta_0 - \int_{L_1}^{L_2} \frac{V_{PI}^2 \epsilon_0 W}{2K(x)\delta(x)^2} dx \quad (3)$$

In Fig. 4(b),  $y_{PI}$  vs.  $V_{PI}$  for Beam1 and Beam 2 is plotted. The analytical solution of Eq. (2) is  $V_{PI} = 315$  Volts for Beam1 and  $V_{PI} = 115$  Volts for Beam2. These values can be compared with the pull-in graphs from FEM analysis in CoventorWare software [6] as superimposed in Fig. 4(b) and listed in Table 2.

#### 3.4 Coupling Beam Design

If the resonators are identical, the passband of the resultant filter will be centered around these resonators's frequency. The coupling beam provides the needed stiffness to shift the resonator frequencies, creating two close resonance modes that form the passband. For a given filter, center frequency  $f$  and bandwidth  $B$ , the required coupling beam stiffness can be found from:

$$K_{cij} = K_e(c)k_{ij} \frac{B}{f} \quad (4)$$

where  $K_{cij}$  is the needed stiffness,  $c$  is the coupling location along the beam length, as can be seen in Fig. 1,  $k_{ij}$

is the normalized coupling coefficient, and  $K_e(c)$  is the resonator stiffness at location  $x_c$  [8]. Using the transmission line theory, the coupling beam is modeled as a T network of mechanical impedances [9]. In this case, half of the mass of the coupling beam is added to each resonator, modeled as series inductors, and its stiffness is modeled as a shunt capacitor as shown in Fig. 7.

$$Ls_a = Ls_b = \frac{1}{2} M_s = \rho T_s W_s L_s$$

$$Cs_c = \frac{1}{Ks_c} = \frac{L_s^3}{6EI_s} \quad (5)$$

where  $L_s$  is the coupling beam length,  $I_s$  is the moment of inertia of the beam and other parameters are shown in Fig. 3(b). The thickness of the structure layer and the minimum width of the coupling beam are usually fixed by fabrication process limitations. From Fig. 3(b) we can see that

$$L_s = \frac{d_s}{2 \cos \theta_s}, R_s = L_s \sin \theta_s \quad (6)$$

Applying the physical limits, equations (4), (5) and (6) are solved simultaneously to find the best values for coupling beam length,  $L_s$ , and angle  $\theta_s$  [4].

The quality factor of the filter is proportional to the ratio of resonator stiffness at the coupling point and coupling beam stiffness. The quality factor of the filter increases when the stiffness of the resonator at coupling beam location increases [4]. By coupling the beams at locations closer to the anchor higher filter quality factor is achievable with same resonator and coupling dimensions.

We used the two beams in Table 1 to create two filters with different center frequencies and coupling locations. The resonator beams, lumped parameters and the correspondent coupling beam dimensions are listed in Tables 3 and 4.

## 4 TEST RESULTS

Adding the coupling beam network and low velocity coupling transformer to the lumped model of a single resonator in Fig. 5, the complete equivalent electrical circuit of filter is constructed as Fig. 7. The micromechanical filter should be terminated with the proper impedance values. Without a proper termination, the filter passband consists of distinct ripples. In Figs. 5 and 7, resistors  $R_{Q1}$  and  $R_{Q2}$  serve this function.

The  $V_{out}/V_{in}$  in frequency domain forms the filter response shape as presented in Figs. 8(a) and 9(a). These plots are based on operation in vacuum condition. The air damping effect is added to the system as a series resistor. Figs 8(b) and 9(b) show the plot of  $dBm(V_{out})$  with respect to frequency in non-vacuum conditions, considering air damping. The fabricated Filters have been testes in air. Figs 8(c) and 9(c) show the  $dBm(V_{out})$  from spectrum analyzer at

output. Comparison between simulation and test result in air show a good agreement, which serves as proof of concept. The center frequencies are as predicted from analytical and FEM analysis.

## 5 CONCLUSIONS

In this paper, a novel V-shape coupling beam was presented which extends the possibility of coupling resonators in lateral direction. It has the advantage of being adjustable with changing V angle to flatten the passband.

A lumped model was derived for fast filter design. Experimental and simulation results were presented to corroborate the modeling and design concept.

## REFERENCES

- [1] C. T. -C. Nguyen, Dig. of Papers, Topical Meeting on Silicon Monolithic Integrated Circuits in RF Systems, Sept. 12-14, 2001, pp. 23-32.
- [2] W.-T. Hsu, J. R. Clark, and C. T.-C. Nguyen, Tech. Dig., IEEE Int. Elect. Devices Meeting, San Francisco, 2000, pp. 493-496.
- [3] David A. Koestar, et. al. "PolyMUMPs Design Handbook," JDS Uniphase Company, Revision 10.
- [4] M. Motiee," MEMS IF/RF Filters," M.A.Sc. thesis, University of Waterloo, 2003.
- [5] Albert park, et. al, J. of Microelectromechanical Sys., Vol. 1, No. 4, Dec. 1992, pp. 179-186.
- [6] www.coventor.com
- [7] M. Motiee, et. al., ASME-IMECE, Washington DC, November 16-21, 2003, # 41568.
- [8] Anatol I. Zverev, "Handbook of Filter Synthesis," John Wiley and Sons, Inc., New York, 1958
- [9] Harrie A. C. Tilmans, J. Mircomech. Microeng., Vol. 6, 1996, pp 157-176, UK.

Beam Sample	$L \mu\text{m}$	$W \mu\text{m}$	$T \mu\text{m}$	$f_0$
Beam 1	100	2	3.5	1.67 MHz
Beam 2	150	2	3.5	723 KHz

Table 1: Dimension of resonators and center frequency.

Beam1				
	$f_0$	Shifted $f$	$M$ (Kg)	$V_{PI}$ (V)
<b>Lumped</b>	1.71MHz	1.69 MHz	6.38E-13	315
<b>FEM</b>	1.70 MHz	1.67 MHz	6.26E-13	277
Beam2				
<b>Lumped</b>	724 KHz	723 KHz	9.58E-13	115
<b>FEM</b>	723 KHz	722 KHz	9.62E-13	95.7

Table 2. Comparison between analytical lumped model and FEM simulation result.

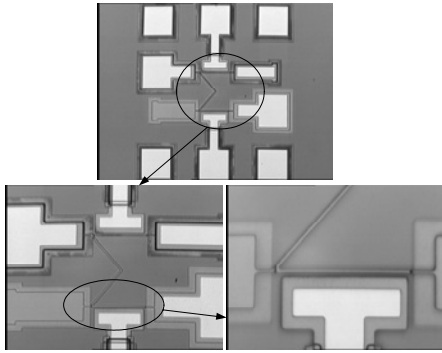


Figure 2: Photo of the fabricated filter sample, Filter1.

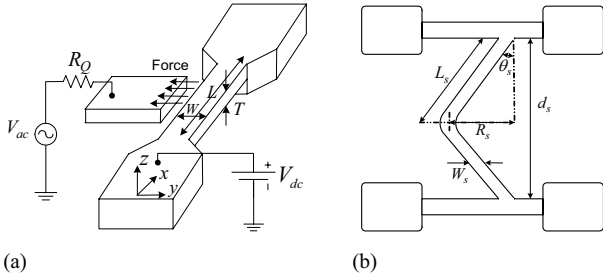


Figure 3: (a) Schematic of a single resonator clamped-clamped beam with proper electrode and bias, (b) coupling beam schematic and dimensions.

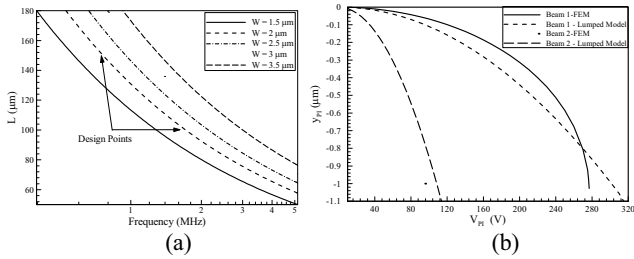


Figure 4: (a) Design curve for clamped-clamped beam in lateral vibration and selected design points, (b) Pull-in voltage graphs for Beam1 and Beam2.

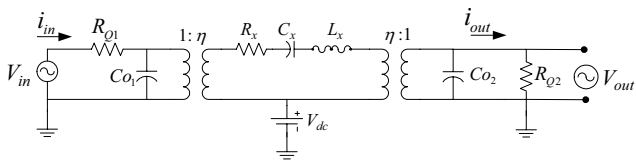


Figure 5: Equivalent lumped circuit for a single resonator.

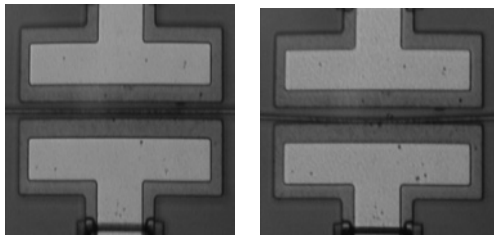


Figure 6: The clamped-clamped beam sample, deformed under pull-in voltage.

Parameter	Filter 1	Filter 2	Units
$C_o$	6.20E-16	8.85E-16	F
$\eta$	3.40E-08	5.07E-08	-
$L_x$	6.38E-13	9.58E-13	H
$C_x$	1.36E-02	4.86E-02	F
$R_x$	3.00E-09	2.50E-09	Ohms
$\eta_c$	8.4	8.4	-
$LS_a=LS_b$	1.85E-12	2.77E-12	F
$CS_c$	6.50E-01	2.27E00	F
$R_Q$	8.5E+05	2.50E+05	KOhms

Table 3: Equivalent lumped parameters, refer to Fig. 7.

Filter	Beam	$L_s$	$R_s$	$\theta_s$	$W_s$	$x_c$
Filter 1	Beam1	115	103	65.15	2	10
Filter 2	Beam1	172	155	64.15	2	15

Table 4: Coupling beam dimensions ( $\mu\text{m}$ )

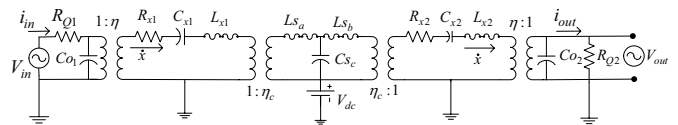


Figure 7: Equivalent lumped model.

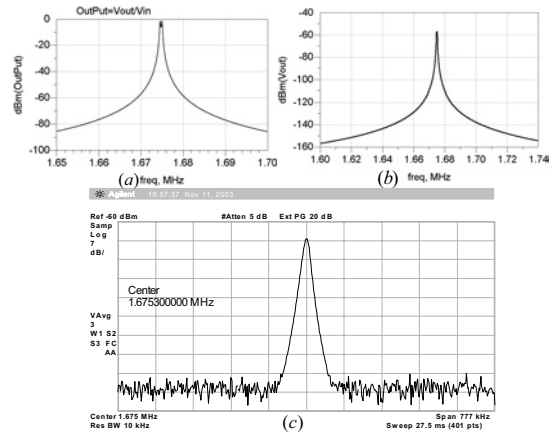


Figure 8: Simulation and test results for Filter1.

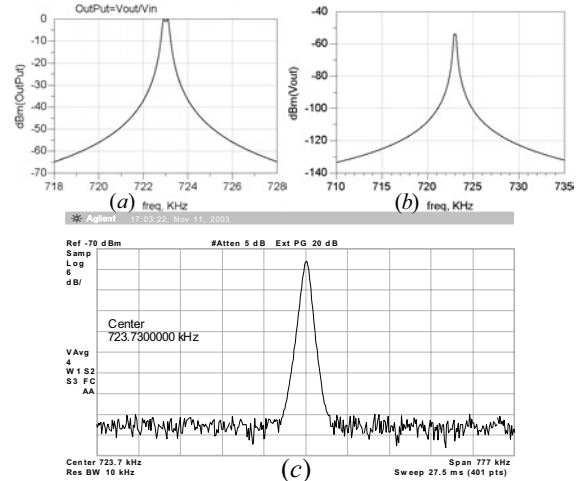


Figure 9: Simulation and test results for Filter2.